

## Influence of Radiation on Non-Darcy Mixed Convection Along a Non-Isothermal Vertical Plate in a Porous Medium With Thermal Dispersion and Viscous Dissipation

Dr. Saddam Atteyia Mohammad

Department of Mechanical Engineering-University of Mosul

### Abstract

A boundary layer analysis is presented for the interaction of non-Darcy mixed convection with thermal radiation along a non-isothermal vertical flat plate embedded in a saturated porous medium with thermal dispersion and viscous dissipation. The governing partial differential equations are transformed into a nonsimilar boundary layer equations. These equations are solved numerically by a finite difference method. The obtained results are checked against previously published work on special case of the problem and is found to be in excellent agreement. A parametric study illustrating the influence of the various physical parameters on velocity and temperature profiles as well as the local Nusselt number are conducted. It is obtained that as the value of the power law index, thermal dispersion parameter, and radiation parameter increases the value of the local Nusselt number increases. As the value of inertia parameter and viscous dissipation parameter increases the value of the local Nusselt number decreases.

**Keywords :** Thermal radiation, Mixed convection, Non-Darcy flow, Vertical plate, Porous medium, Thermal dispersion, Viscous dissipation, Nonsimilarity solution.

### تأثير الإشعاع على الحمل المختلط اللادارسي على طول صفيحة عمودية غير ثابتة درجة الحرارة في وسط مسامي مع التشتت الحراري والتبدد اللزج

د. صدام عطية محمد

قسم الهندسة الميكانيكية-جامعة الموصل

### الخلاصة

لقد تم في هذا البحث عرض تحليل للطبقة المتاخمة الناتجة من تفاعل الحمل المختلط اللادارسي مع الإشعاع الحراري على طول صفيحة مستوية عمودية غير ثابتة درجة الحرارة مغمورة في وسط مسامي مشبع مع التشتت الحراري والتبدد اللزج. لقد تم تحويل المعادلات الاشتقاقية الجزئية المتحكمة بالمسألة إلى معادلات للطبقة المتاخمة بالصيغة اللامتماثلة. إن هذه المعادلات تم حلها عددياً باستخدام طريقة الفرق المحدود. لقد تم مقارنة النتائج الحالية مع نتائج عمل سابق مطبوع على حالة خاصة للمسألة ووجد أن هناك تطابق ممتاز بين الحلين. تم إجراء دراسة استدلالية لغرض توضيح تأثير المعلمات الفيزيائية المختلفة على المظاهر الجانبية للسرعة ودرجة الحرارة بالإضافة إلى عدد نسلت الموقعي. لقد وجد انه بزيادة قيمة أس قانون القوة، معلمة التشتت الحراري، ومعلمة الإشعاع الحراري فان قيمة عدد نسلت الموقعي ستزداد. ووجد انه بزيادة قيمة معلمة القصور الذاتي ومعلمة التبدد اللزج فان قيمة عدد نسلت الموقعي سوف تقل.

Received: 22 – 9 - 2013

Accepted: 7 – 4 - 2014

## Nomenclature

$a$	Constant, equation (9).	$T$	Temperature ( $K$ ).
$c_p$	Specific heat of the fluid ( $J/kg.K$ ).	$u$	Velocity components in the $x$ direction ( $m/s$ ).
$C$	Inertial coefficient.	$U_\infty$	Free stream velocity ( $m/s$ ).
$d$	Mean particle diameter.	$v$	Velocity components in the $y$ direction ( $m/s$ ).
$D$	Dimensionless thermal dispersion parameter.	$V$	Dimensionless viscous dissipation parameter.
$f$	Dimensionless stream function.	$x, y$	Axial and normal coordinate ( $m$ ).
$g$	Gravitational acceleration ( $m/s^2$ ).	$\alpha$	Molecular thermal diffusivity ( $m^2/s$ ).
$h$	Local heat transfer coefficient ( $W/m^2.K$ ).	$\alpha_d$	Dispersion thermal diffusivity ( $m^2/s$ ).
$i$	Index of mesh points in the $\zeta$ -direction.	$\beta$	Thermal expansion coefficient of the fluid ( $1/K$ ).
$I$	Dimensionless inertia coefficient.	$\gamma$	Constant, equation (6).
$j$	Index of mesh points in the $\eta$ -direction.	$\zeta, \eta$	Subintervals in the $\zeta$ and $\eta$ direction.
$k$	Thermal conductivity of fluid ( $W/m.K$ ).	$\zeta$	Nonsimilarity parameter.
$k_d$	Dispersion thermal conductivity ( $W/m.K$ ).	$\eta$	Pseudosimilarity variable.
$k$	Mean absorption coefficient ( $1/m$ ).	$\theta$	Dimensionless temperature.
$K$	Permeability of the porous medium ( $m^2$ ).	$\mu$	Dynamic viscosity of the fluid ( $kg/s.m$ ).
		$\nu$	Kinematic viscosity of fluid ( $m^2/s$ ).
$n$	Constant, equation (9).	$\rho$	Density of the fluid ( $kg/m^3$ ).
$Nu_x$	Local Nusselt number.		
$N_\zeta, N_\eta$	Integer numbers greater than zero.		Prefix indicating summation.
$P$	Pressure of the fluid ( $N/m^2$ ).	$\psi$	Stream function.
$Pe_x$	Local Peclet number.		
$q_r$	Radiation heat flux ( $W/m^2$ ).	$\sigma$	Stefan-Boltzmann constant ( $W/m^2.K^4$ ).
$q_w$	Local surface heat flux ( $W/m^2$ ).		
$R$	Dimensionless radiation parameter.		
$Ra_x$	Local Rayleigh number.		
<b>Subscript</b>			
$max$	Sufficiently large value.	$old$	Old value.
$na$	Assumed value not affected by the first convergence criterion.	$w$	Surface conditions.
$new$	New value.		Conditions far away from surface.

## **Introduction**

The corresponding problem of convective heat transfer in a saturated porous medium has many important applications in geothermal and geophysical engineering [1]. Most early studies on porous media have used the Darcy law which is limited to slow flows. However, for high velocity flow situations, the Darcy law is inapplicable since it does not account for the resulting inertia effects of the porous medium. A secondary effect of a porous medium on the flow appears as a result of mixing and recirculation of local fluid particles through tortuous paths formed by the porous medium solid particles. This effect is classified as thermal dispersion [2]. Viscous dissipation can be relevant if high viscous fluids with a low thermal conductivity are considered [3]. Viscous dissipation which features as a source term in the fluid flow, manifests itself as an appreciable rise in fluid temperature due to conversion of kinetic motion of the fluid to thermal energy [4]. Thermal radiation is one of the many factors that control heat transfer in a non-isothermal system. Many researchers have considered the effect of radiation on mixed convection in porous media by using the Rosselant diffusion approximation.

Below some of the previous studies about mixed convection along a vertical plate embedded in a uniform porous medium. Yih [1] used a boundary layer analysis to investigate the heat and mass transfer characteristics for prescribed surface temperature/concentration or prescribed heat/mass flux. It was found that the local heat and mass transfer rates increase with increasing the exponent of prescribed surface temperature/concentration and the exponent of prescribed heat/mass flux and buoyancy parameter. For both boundary conditions increasing buoyancy ratio increases the local heat and mass transfer rates. It is apparent that Lewis number has a pronounced effect on the local mass transfer rate than it does on the local heat transfer rate. Furthermore, increasing Lewis number decreases (increases) the local heat (mass) transfer rate.

Chamkha and Khaled [2] investigated the problem of hydromagnetic simultaneous heat and mass transfer with a stratified free stream and in the presence of thermal dispersion for power-law variations of wall temperature and concentration. It was found that while the local Nusselt number decreased as a result of the presence of either the magnetic field, negative free stream temperature stratification or positive wall mass transfer, it increased due to imposition of both negative wall mass transfer and free stream temperature stratification. Also, the Nusselt number was increased due to the presence of heat absorption effect. In addition, the Nusselt number decreased as a result of considering the porous medium inertia effects. Furthermore, increasing the ratio of concentration to thermal buoyancies was found to cause enhancements in the values of the Nusselt number and the Sherwood number. Finally, thermal dispersion was found to increase the rate of heat transfer from the plate.

Chamkha [5] derived continuum boundary layer equations for governing hydromagnetic flow along a permeable plate maintained at constant heat flux with heat generation and magnetic dissipation. It was found that both the skin friction group and the wall heat transfer group decreased along the plate for the forced convection dominated regime, while they increased for the buoyancy dominated regime. In addition, reductions in both the skin friction group and the wall heat transfer group were observed as either the Hartmann number, inverse Darcy number, or dimensionless porous medium inertia coefficient was increased. Furthermore, increasing the heat generation coefficient or reducing the fluid's Prandtl number produced lower wall heat transfer group values, while the skin friction group was increased as either of these parameters was increased. Tashtoush and Kodah [6] made an analytical study for wall effects in non-Darcy flow. It was found that increasing mixing

parameters increases the rate of heat transfer and increases the velocity within the boundary layer due to induced-favorable pressure gradient. The non-Darcian effects tend to decrease the velocity within the boundary layer, and broaden the temperature distribution, which results in lower heat transfer rate at higher values of these effects.

Kodah and Al-Gasem [7] presented nonsimilarity solutions for non-Darcy flow for variable surface heat flux. It was found that increasing mixing parameters increases the rate of heat transfer and increases the velocity within the boundary layer due to induced-favourable pressure gradient. Also, increasing the exponent of the power-law form heating boundary conditions will decrease the velocity within the boundary layer, and increase the rate of heat transfer. The non-Darcian effects tend to decrease the velocity within the boundary layer, and broaden the temperature distributions, which result in lower heat transfer rate at higher value of this effect (inertia forced effect). Gorla and Kumari [8] presented a nonsimilar boundary layer analysis for power-law type non-Newtonian fluids with power-law wall temperature distribution. It was obtained that the thermal boundary layer thickness decreases as the nonsimilarity parameter for forced convection increases. The slip velocity at the porous surface decreases as the viscosity index increases. The surface temperature gradient and hence the heat transfer rate increases as the nonsimilarity parameter for forced convection increases. The slip velocity at the wall increases as the nonsimilarity parameter for forced convection increases. For local Nusselt number it is observed that the solutions for the forced convection dominated regime and the free convection dominated regime meet and match over the mixed convection regime. As the index of power-law wall temperature distribution and the nonsimilarity parameter for forced convection increase, the Nusselt number increases for a given value of viscosity index. As the value of the viscosity index increases, the heat transfer rate parameter decreases.

Hassanien, et al. [9] presented a boundary layer analysis and the effects of thermal dispersion and stratification on the flow and temperature fields are investigated. It was concluded that Nusselt number increases with the stratified parameter. For given values of wall temperature exponent, stratification parameter and dispersion parameter the slip velocity decreases as the buoyancy parameter increases, but does not vary significantly with different values of dispersion. The values of the velocity increase as the dispersion parameter decreases. The temperature distribution with given values of wall temperature exponent and stratification parameter revealed that the effect of buoyancy increases the values of temperature within the boundary layer. For the forced convection dominated region the slip velocity decreases as the buoyancy parameter increases or the inertial parameter decreases. The temperature within the boundary layer increases with the dispersion parameter, the buoyancy parameter and the inertial parameter. Murthy [10] considered an isothermal vertical wall and the effects of thermal dispersion and viscous dissipation in both aiding and opposing flows are analyzed. Series solution is obtained, first and second order effects of dissipation revealed that viscous dissipation lowers the heat transfer rate. Observations also revealed that the thermal dispersion effect enhances the heat transfer rate and the effect of viscous dissipation is observed to increase with increasing values of the dispersion parameter.

Chamkha and Khaled [11] considered hydromagnetic simultaneous heat and mass transfer over a permeable plate for power-law variations of both the wall temperature and concentration and the wall heat flux and mass flux. It was found that for both prescribed wall temperature and concentration conditions and prescribed wall heat and mass flux conditions while local Nusselt number decreased as a result of the presence of either the magnetic field or positive surface blowing, it increased due to imposition of both surface suction and larger values of power law indices. Also, Nusselt number was increased due to the presence of heat

absorption effects. Furthermore, increasing the ratio of concentration to thermal buoyancies was found to cause enhancements in the values of Nusselt and Sherwood numbers. Finally, porous medium inertia effect were found to decrease local Nusselt number. Tashtoush [12] introduced a new analytical solution for the effect of viscous dissipation about an isothermal wall in Darcy and non-Darcy porous media for both the aiding and opposing flows using Gebhart number. It was found from the Nusselt number results that viscous dissipation lowers the heat transfer rate in both Darcy and Forchheimer flow regimes for aiding as well as opposing flows.

Hassanien and Omer [13] performed an analysis for the heating condition of power-law variation in wall temperature. No-slip boundary condition, the variation of permeability and thermal conductivity are taken into consideration. It was found that as the mixed convection parameter decreases from the pure forced convection limit to the pure free convection limit, the thermal boundary layer thickness increases first and then decreases, whereas the local Nusselt number decreases first and then increases. The results clearly indicate that the local Nusselt number increases with increasing value of the index of power-law wall temperature distribution for a given mixed convection parameter for both uniform and variable permeability cases. In comparison to uniform permeability, the variable permeability is found to have higher local heat transfer. Chamkha, et al. [14] investigate the combined effects of buoyancy, porous inertial drag, boundary vorticity diffusion (Brinkman friction), transverse magnetic field, viscous dissipation, wall transpiration, thermal conductivity and various other thermofluid parameters on the convection boundary layer flow of an electrically-conducting fluid past a permeable plate. It was concluded that generally, local skin friction function is increased in magnitude by rising Grashof number, suction, positive Eckert number, and Darcy and Forchheimer numbers; conversely rising Hartmann magnetic number, thermal conductivity ratio, Prandtl number, Reynolds number, and blowing, and negative Eckert number all reduce local shear stresses. Local Nusselt number function is increased in magnitude by increasing Grashof number, suction, negative Eckert number, rising Darcy number, Forchheimer number, thermal conductivity ratio, Prandtl number, and depressed by increasing blowing, Hartmann magnetic number, positive Eckert number, and Reynolds number.

Murthy, et al. [15] considered mixed convection flow of an absorbing fluid up a non-Darcy porous medium supported by an ideally transparent plate due to solar radiation. The effect of the radiation parameter with fluid suction/injection is analyzed in both aiding and opposing flow. It is observed that in the aiding flow, the effect of thermal radiation is to (i) increase the convective moment in the boundary layer, (ii) increase the thermal boundary-layer thickness with an increase in the value of the radiation parameter, (iii) enhance the heat transfer coefficient in the medium. Also the effect of radiation is more predominant in the near-Darcy region than in the non-Darcy region. Fluid suction decreased the thickness of the thermal boundary layer and enhanced the heat transfer into the medium whereas fluid injection increased the boundary-layer thickness and reduced the heat transfer into the medium, due to thermal radiation effects, and the heat transfer coefficient is increased in both the suction and injection regions. In the opposing flow, separation is seen to depend on the flow governing parameter and also on the inertial parameter. The thermal boundary-layer thickness increased with increasing value of the radiation parameter thereby reducing the heat transfer into the medium. The heat transfer coefficient increased with an increase in the value of the radiation parameter and also as the value of the surface mass flux parameter moves from the injection region to the suction region.

Mohammadein and El-Shaer [16] studied mixed convection flow incorporating the variation of permeability and thermal conductivity. It was revealed that an increase in the parameter  $Gr/Re^2$  or  $\alpha/\sigma Re$  (where  $Gr$ ,  $Re$ ,  $\alpha$ , and  $\sigma$  are Grashof number, Reynolds number, ratio of viscosities, and permeability parameter respectively) leads to increase in the skin friction and rate heat transfer but greater viscous dissipative heat causes arise in the skin friction and fall in the rate of heat transfer. The velocity profile increases as  $Gr/Re^2$  or  $\alpha/\sigma Re$  and the ratio of thermal conductivity of the solid to the liquid increase and it decreases as Prandtl number increases. An decrease in the parameter  $Gr/Re^2$  or  $\alpha/\sigma Re$  enhances the temperature, while it reduces as the ratio of thermal conductivity of the solid to the liquid increases. This increment is much higher for variable permeability case than uniform permeability one. Reddy and Reddy [17] study the effects of radiation on heat and mass transfer flow of a viscous incompressible electrically conducting and radiating fluid over an isothermal vertical porous plate. It was found that as the magnetic parameter increases, the velocity decreases. The velocity decreases as the permeability parameter increases. The velocity profiles decrease monotonically with the increase of suction parameter. An increase in the radiation parameter results in increasing velocity within the boundary layer. Increasing values of Prandtl number results in a decreasing velocity. When the heat is generated the buoyancy force increases which induces the flow rate to increase giving rise to the increase in the velocity profiles. The velocity slightly decreases with an increase in Schmidt number. The temperature decreases as the suction parameter increases. An increase in the radiation parameter results in increasing temperature within the boundary layer. An increase in Prandtl number results in a decrease of the thermal boundary layer and in general lower average temperature within the boundary layer. The temperature increases as the heat generation parameter increases. The concentration decreases as the suction parameter or Schmidt number increases. As the magnetic parameter or permeability parameter increases, there is a fall in the skin-friction coefficient, the Nusselt number and the Sherwood number. As the suction parameter increases, the skin-friction coefficient decreases, while the Nusselt number and Sherwood number increase. As the radiation parameter increases, the skin-friction reduces and the Nusselt number increases, but the Sherwood number remains unchanged. As the Prandtl number increases, both the skin-friction coefficient and Sherwood number decrease, where as the Nusselt number increases. The increase in the heat generation parameter leads to a rise in the skin-friction coefficient and Sherwood number while a fall in the Nusselt number. As the Schmidt number increases, there is a fall in the skin-friction coefficient and Nusselt number while a rise in the Sherwood number.

Hsieh, et al. [21] analyzed the problem of mixed convection about a vertical flat plate embedded in a porous medium. Nonsimilarity solutions are obtained for the cases of variable wall temperature (VWT) and variable surface heat flux (VHF). The entire mixed convection regime is covered by two different nonsimilarity parameters for VWT and VHF cases. It was found that as the nonsimilarity parameters decreases from pure forced convection limit to pure free convection limit, the thermal boundary layer thickness increases first and then decreases, but the local Nusselt number for both cases of surface heating conditions decreases first and then increases. The correlation equations for the local and average Nusselt numbers are also obtained for the two surface heating conditions. Narayana et al. [22] presents an investigation of the influence of thermal radiation and viscous dissipation on the mixed convection flow due to an isothermal vertical plate immersed in a non-Darcy porous medium saturated with a Newtonian fluid. The ambient temperature is assumed to vary linearly with the distance from the origin. It was found that velocity and temperature profiles are significantly affected by viscous dissipation and thermal radiation parameters. The combined

and individual effects of dissipation parameter and thermal radiation parameter is to increase the temperature gradient at the surface and thereby contribute to reduce the rate of heat transfer.

Previous works don't take into consideration the effects of radiation on non-Darcy mixed convection along a vertical plate with thermal dispersion and viscous dissipation. Therefore, in this work, a boundary layer analysis will be presented for the interaction of non-Darcy mixed convection with thermal radiation along a non-isothermal vertical flat plate embedded in a saturated porous medium with thermal dispersion and viscous dissipation.

## Analysis

Consider the steady, incompressible, laminar, two-dimensional mixed convection boundary layer flow along an non-isothermal vertical flat plate embedded in a fluid saturated porous medium as shown in Figure (1). The axial and normal coordinates are  $x$  and  $y$ . The flow is assumed to be in the  $x$ -direction. The gravitational acceleration  $g$  is acting downward in the direction opposite to the  $x$ . For low permeability and porosity the viscous resistance due to the solid boundary is small and can therefore be neglected. Experimental observations indicate that pressure drop is proportional to a linear combination of flow velocity and the square of this velocity [12]. The radiative heat flux in the  $x$  direction is considered negligible in comparison with that in the  $y$  direction. The fluid is assumed to be gray, emitting, and absorbing radiation but non-scattering medium. The surface temperature  $T_w$  is higher than the corresponding value  $T_\infty$  sufficiently far away from the flat surface. The properties of the fluid and the porous media, such as viscosity, thermal conductivity, specific heat and permeability, all are assumed to be constant, except the density in the buoyancy term of the balance of the momentum equation that is approximated according to the Boussinesq approximation. The governing boundary layer equations are:

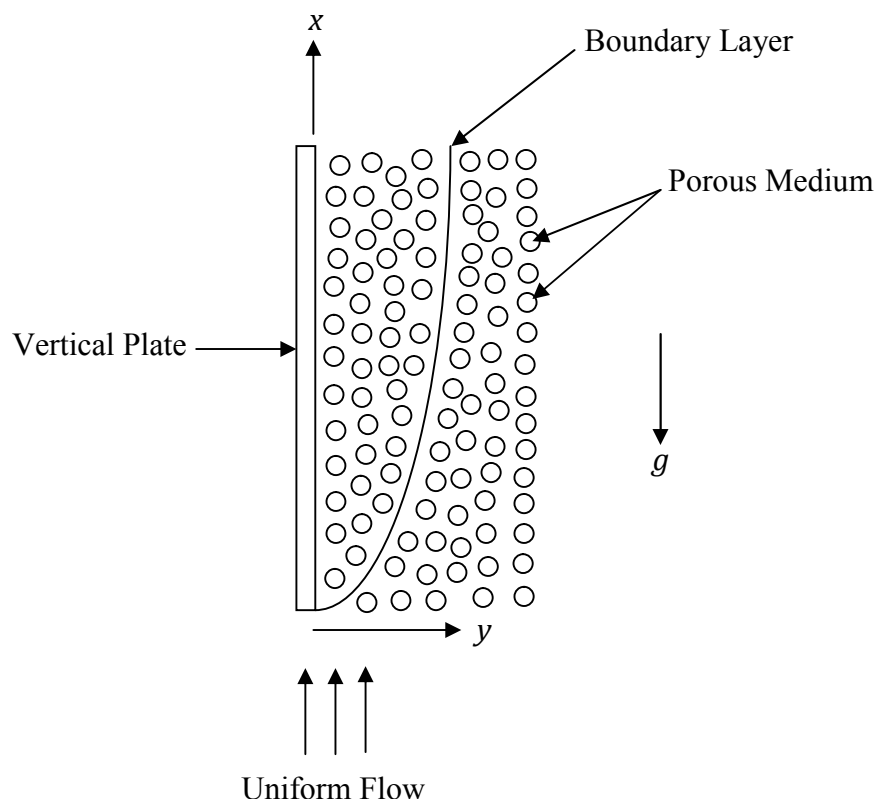
1- Continuity equation.

$$\frac{\partial u}{\partial x} + \frac{\partial v}{\partial y} = 0 \quad (1)$$

Where  $u$  and  $v$  are the velocity components in the  $x$  and  $y$  directions respectively.

2- Momentum equation [18,20].

a. In the  $x$ -direction



Figure(1): Physical model and coordinate system.

$$u = -\frac{K}{\mu} \left( \frac{\partial P}{\partial x} + \rho g \right) - \frac{c\sqrt{K}}{\nu} u^2 \quad (2)$$

b. In the  $y$ -direction

$$v = -\frac{K}{\mu} \left( \frac{\partial P}{\partial y} \right) - \frac{c\sqrt{K}}{\nu} v^2 \quad (3)$$

Eliminate pressure term from equations (2) and (3) by differentiating equation (2) with respect to  $y$  and equation (3) with respect to  $x$ . Invoking the Boussinesq approximation  $\rho = \rho_\infty [1 - \beta(T - T_\infty)]$  [18] and the assumption that within the boundary layer ( $v \ll u$ ,  $\frac{\partial}{\partial x} \gg \frac{\partial}{\partial y}$ ). Therefore, the single form of the momentum equation will be as follows :

$$\left[ 1 + \frac{2c\sqrt{K}}{\nu} u \right] \frac{\partial u}{\partial y} - \frac{K g \beta}{\nu} \frac{\partial T}{\partial y} = 0 \quad (4)$$

3- Energy equation.

$$u \frac{\partial T}{\partial x} + v \frac{\partial T}{\partial y} = \frac{\partial}{\partial y} \left[ (\alpha + \alpha_d) \frac{\partial T}{\partial y} \right] - \frac{1}{\rho c_p} \frac{\partial q_r}{\partial y} + \frac{\nu}{K c_p} u \left( u + \frac{c\sqrt{K}}{\nu} u^2 \right) \quad (5)$$

$\alpha_d$  can be represented as a linear relation of the fluid velocity as follows [2,9,10]

$$\alpha_d = \gamma u d \quad (6)$$

The value of  $\gamma$  is to be determined from the experiments, it is observed that its values lies between  $\frac{1}{7}$  and  $\frac{1}{3}$  [10]. For all calculations, it will be considered  $\gamma = 0.3$  in the present study.

4- Radiative heat flux.

The radiative heat flux term  $q_r$  is written using the Rosseland approximation [15,17]

$$q_r = -\frac{4\sigma}{3k} \frac{\partial T^4}{\partial y} \quad (7)$$

By using equation (7), the present analysis is limited to optically thick fluids. If the temperature differences within the flow are sufficiently small, then  $T^4$  may be expressed as a linear function of temperature [17]

$$T^4 = 4T_\infty^3 T - 3T_\infty^4 \quad (8)$$

5- Boundary conditions [11].

$$\begin{aligned} y = 0 \quad v = 0 \quad T = T_w(x) = T_\infty + ax^n \\ y \quad u = U_\infty \quad T = T_\infty \end{aligned} \quad (9)$$

6- Dimensionless variables.

To facilitate the present analysis, the system of equations (4) and (5) will be transformed into dimensionless form by introducing [13]

$$\zeta = \left[ 1 + \left( \frac{Ra_x}{Pe_x} \right)^{1/2} \right]^{-1} \quad \eta = \frac{y}{x} Pe_x^{1/2} \zeta^{-1} \quad (10)$$

$$f(\zeta, \eta) = \frac{\psi}{\alpha Pe_x^{1/2} \zeta^{-1}} \quad \theta(\zeta, \eta) = \frac{T - T_\infty}{T_w - T_\infty} \quad (11)$$

Where  $\zeta$  is the nonsimilarity mixed convection parameter. The entire mixed convection regime is covered by the parameter  $\zeta$  from pure free convection limit ( $\zeta = 0$ ) to the pure forced convection limit ( $\zeta = 1$ ).  $\eta$  is the pseudosimilarity variable,  $f$  is the dimensionless stream function,  $\theta$  is the dimensionless temperature,  $Pe_x = U_\infty x / \alpha$  is the local Peclet number,  $Ra_x = g\beta[T_w(x) - T_\infty]Kx / \nu\alpha$  is the local Rayleigh number, and  $\psi$  is the stream function defined by  $u = \partial\psi/\partial y$  and  $v = -\partial\psi/\partial x$  such that the continuity equation is automatically satisfied. Applying the transformation of variables (10) and (11) to the governing equations (4) and (5) leads to :

7- Dimensionless momentum equation.

$$[1 + 2If]f'' - (1 - \zeta)^2\theta' = 0 \quad (12)$$

Where  $I = \frac{c\bar{k}\alpha}{\nu x} (Pe_x^{1/2} + Ra_x^{1/2})^2$  is the dimensionless porous medium inertia coefficient.

8- Dimensionless energy equation.

$$\left[ 1 + \gamma Df' + \frac{4}{3}R \right] \theta'' + \left[ \frac{1}{2}(1 + n(1 - \zeta))f + \gamma Df' \right] \theta' - nf'\theta = \frac{n}{2}\zeta(\zeta - 1) \left[ f' \frac{\partial\theta}{\partial\zeta} - \theta \frac{\partial f}{\partial\zeta} \right] - V[(f')^2 + I(f')^3] \quad (13)$$

Where  $D = \frac{d}{x} (Pe_x^{1/2} + Ra_x^{1/2})^2$  is the thermal dispersion parameter,  $R = 4\sigma T_\infty^3 / k$   $k$  is the radiation parameter, and  $V = \frac{\nu\alpha}{Kc_p\Delta T} (Pe_x^{1/2} + Ra_x^{1/2})^2$  is the viscous dissipation parameter.

9- Dimensionless boundary conditions.

$$\begin{aligned} \eta = 0 \quad f = 0 \quad \theta = 1 \\ \eta \quad f' = \zeta^2 \quad \theta = 0 \end{aligned} \quad (14)$$

10- Local Nusselt number.

The local Nusselt number is defined as  $Nu_x = hx/k$  where the local heat transfer coefficient  $h = q_w / [T_w(x) - T_\infty]$  and  $q_w = - \left[ (k + k_d) \frac{\partial T}{\partial y} \Big|_{y=0} + \frac{16\sigma T_\infty^3}{3k} \frac{\partial T}{\partial y} \Big|_{y=0} \right]$ . In terms of the new variables, this quantity have the expression :

$$\frac{Nu_x}{Pe_x^{1/2} \zeta^{-1}} = - \left[ 1 + \gamma Df'(\zeta, 0) + \frac{4}{3}R \right] \theta'(\zeta, 0) \quad (15)$$

Another physical quantities of interest include the velocity components  $u$  and  $v$  in the  $x$  and  $y$  directions, in terms of the new variables have the expressions :

$$u = \frac{U_\infty}{\zeta^2} f \quad (16)$$

$$v = -\frac{\alpha}{x} Pe_x^{1/2} \frac{1}{\zeta} \left\{ \frac{1}{2} [1 + n(1 - \zeta)] f - \frac{1}{2} [1 - n(1 - \zeta)] \eta f' - \frac{1}{2} n \zeta (1 - \zeta) \frac{\partial f}{\partial \zeta} \right\} \quad (17)$$

The primes in equations (12-17) denote partial differentiation with respect to  $\eta$  and the presence of  $\partial/\partial\zeta$  makes them nonsimilar.

## Numerical Method

Numerical method adopted to solve the system of nonlinear equations (12 and 13) is based on the following concepts [19] :

- 1-  $\eta$  in the boundary conditions are replaced by  $\eta = \eta_{max}$  where  $\eta_{max}$  is a sufficiently large value of  $\eta$  where the boundary conditions (14) for velocity is satisfied.
- 2- The domain  $(\zeta, \eta)$  is discretized with an equispaced mesh in the  $\zeta$  direction ( $\Delta\zeta = 0.1$ ) and another equispaced mesh in the  $\eta$  direction ( $\Delta\eta = 0.02$ ).
- 3- All the partial derivatives are evaluated by the central difference approximation. When  $\zeta = 0$  and  $\zeta = 1$  the central difference approximation for the partial derivatives with respect to  $\zeta$  vanish.
- 4- Due to the nonlinearity of the equations two iteration loops based on the successive substitutions are used.
- 5- In each inner iteration loop, the value of  $\zeta$  is fixed, while each of equations (12) and (13) is solved as a linear second-order boundary-value problem of ordinary differential equation on the  $\eta$  domain. The inner integration is continued until the nonlinear solution converges.
- 6- In the outer iteration loop, the value of  $\zeta$  is advanced from 0.1 to 0.9. After every outer iteration loop the derivatives with respect to  $\zeta$  are updated.

The system of dimensionless equations are programmed by using Fortran language. The program obtains the solution of pure free convection, pure forced convection, and mixed convection respectively. A convergence criterion of  $\sum_{j=1}^{N_\eta} |f_{new}(j, i) - f_{old}(j, i)| < 0.001$  is adopted in this work for all convection types. Where the subscripts (new) and (old) refer to the new and old values of  $f$ . As well as the above convergence criterion there is another one on the whole region of mixed convection that is :

For  $i = 1, \dots, N_\zeta$

$$\sum_{j=1}^{N_\eta} |f_{new}(j, i) - f_{na}(j, i)| < 0.001$$

If (yes) then next  $i$ . If (no) then updates the values of dimensionless stream function and dimensionless temperature for mixed convection region. Then repeat the solution process for this region. Where the subscript (na) refer to the assumed value of the dimensionless stream function that is not affected by the first convergence criterion.

## Results and Discussion

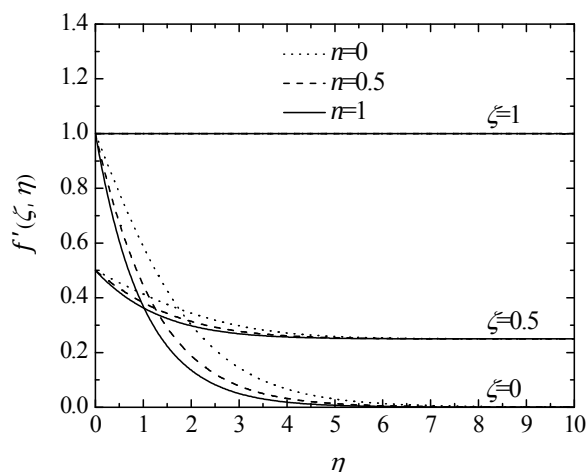
The accuracy of the aforementioned numerical method was validated by direct comparison with the numerical results reported earlier by Hsieh et al. [21] for the case of Darcy solution. In tabulated form the comparison of  $Nu_x (Pe_x^{1/2} \zeta^{-1})$  values is shown in

Table (1). In graphical form the comparison is illustrated in Figure (4). It can be seen from this comparison that there is an excellent agreement between the results.

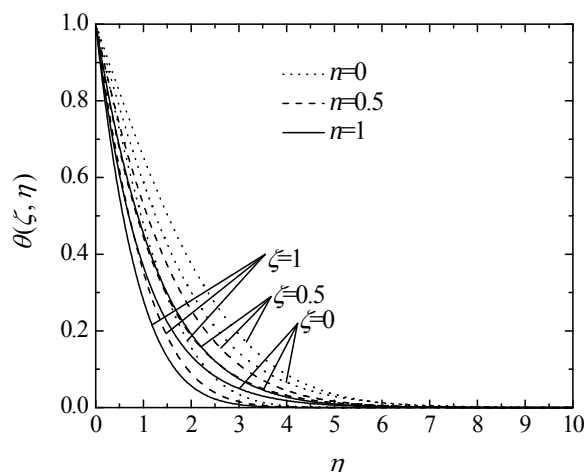
**Table (1):** Comparison values of  $Nu_x / (Pe_x^{1/2} \zeta^{-1})$  at values of  $\zeta$  and  $n$ .

$\zeta$	Hsieh et al. [21]			Present results		
	$n=0$	$n=0.5$	$n=1$	$n=0$	$n=0.5$	$n=1$
0	0.4438	0.7704	1	0.4442	0.7708	1.0004
0.1	0.4035	0.6991	0.9071	0.4039	0.6991	0.9069
0.2	0.3732	0.6419	0.8314	0.3736	0.6418	0.8311
0.3	0.355	0.6026	0.7783	0.3553	0.6024	0.7779
0.4	0.3506	0.5844	0.7522	0.3506	0.584	0.7516
0.5	0.3603	0.589	0.7555	0.3603	0.5886	0.7548
0.6	0.3832	0.616	0.7877	0.3832	0.6157	0.7872
0.7	0.4174	0.6629	0.8457	0.4174	0.6627	0.8454
0.8	0.4603	0.7259	0.925	0.4603	0.7259	0.9248
0.9	0.5098	0.8014	1.0206	0.5099	0.8015	1.0205
1	0.5642	0.8862	1.1284	0.5642	0.8863	1.1284

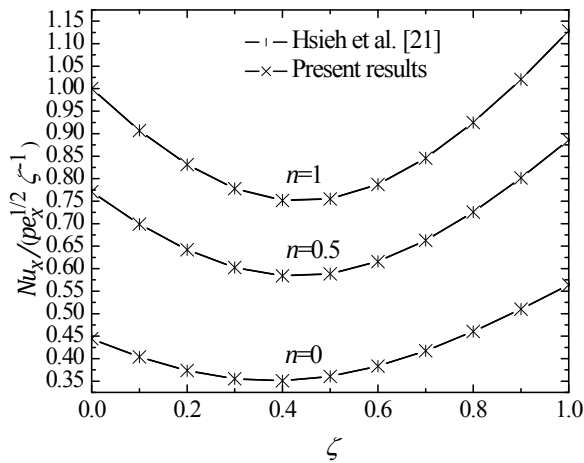
**Effect of constant :** Figures (2) and (3) illustrates the influence of various values of the power law index  $n$  and  $\zeta$  on the velocity and temperature profiles respectively. It can be observed that as  $n$  increases the velocity of the fluid decreases and the temperature gradient increases. This, in turn, results in increasing the convective heat transfer rate. Therefore the local Nusselt number increases as  $n$  increases as shown in Figure (4).



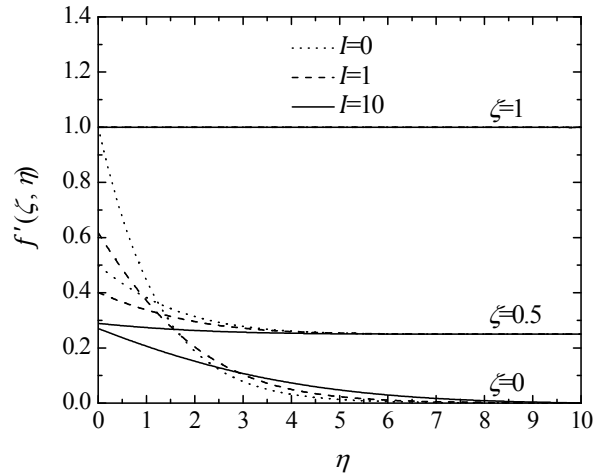
**Figure(2):** Effect of  $n$  and  $\zeta$  on the velocity profile ( $I=D=R=V=0$ ).



**Figure(3):** Effect of  $n$  and  $\zeta$  on the temperature profile ( $I=D=R=V=0$ ).

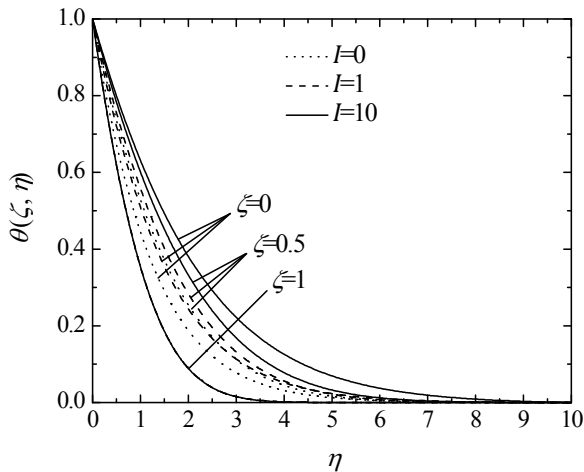


**Figure(4):** Effect of  $n$  and  $\zeta$  on the local Nusselt number ( $I=D=R=V=0$ ).

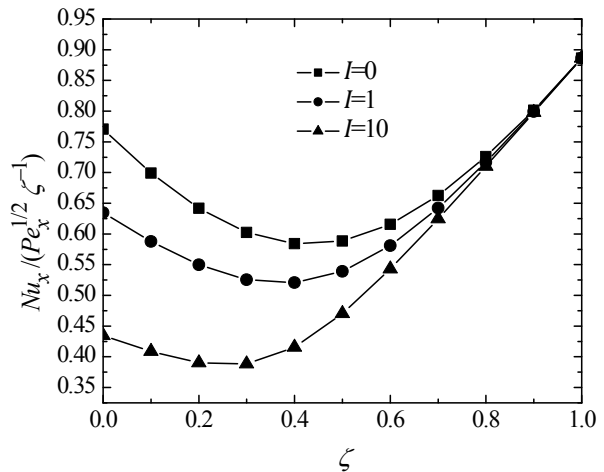


**Figure(5):** Effect of  $I$  and  $\zeta$  on the velocity profile ( $n=0.5, D=R=V=0$ ).

**Effect of  $I$ :** Figures (5) and (6) displays the effect of inertia parameter  $I$  and  $\zeta$  on the velocity and temperature profiles respectively. As  $I$  increases the velocity of fluid and the



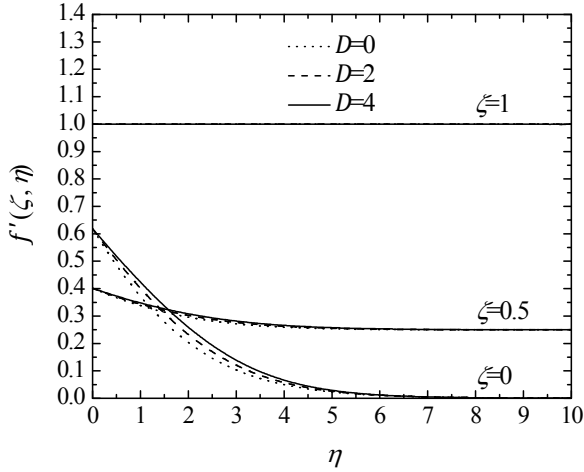
**Figure(6):** Effect of  $I$  and  $\zeta$  on the temperature profile ( $n=0.5, D=R=V=0$ ).



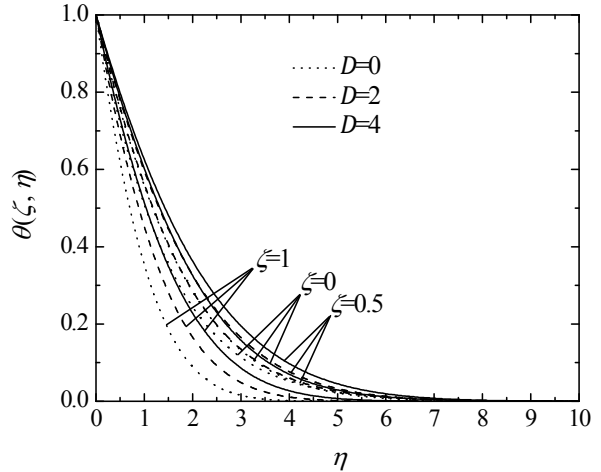
**Figure(7):** Effect of  $I$  and  $\zeta$  on the local Nusselt number ( $n=0.5, D=R=V=0$ ).

temperature gradient decreases. Figure (7) depicts the effect of inertia parameter on the local Nusselt number. It is clear that the local Nusselt number decreases as  $I$  increases and this effect is small for large values of  $\zeta$ . The physical reason for the above effect is that, additional resistance against the flow is introduced because of the porous medium inertia effect. This results in decreasing the enthalpy of the flow streams. Furthermore, it should be noted that the inertia of the porous medium produces no effect for the case of forced convection ( $\zeta = 1$ ). This is because the model of the problem does not take into account the no-slip velocity boundary conditions.

**Effect of  $D$  :** The effect of thermal dispersion parameter  $D$  and  $\zeta$  on the velocity and temperature profiles are shown in Figures (8) and (9) respectively. Increasing the thermal dispersion parameter results in an increase in the thermal diffusion, and as a result, the flow velocity and fluid temperature increases. This, in turn, results in increasing the rate of heat

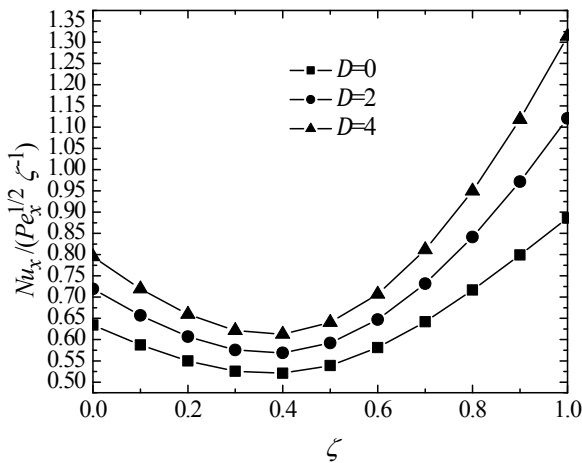


**Figure(8):** Effect of  $D$  and  $\zeta$  on the velocity profile ( $n=0.5, I=1, R=V=0$ ).

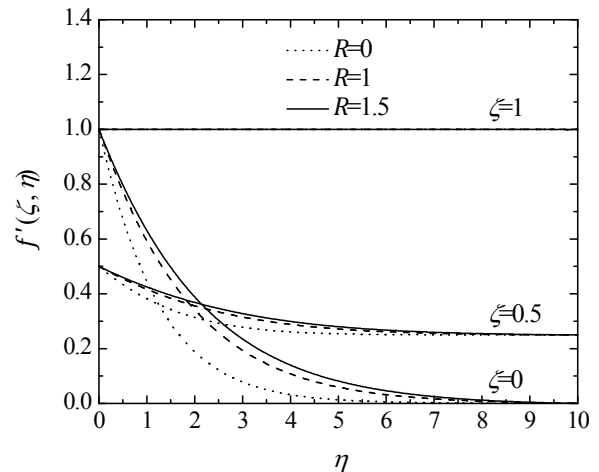


**Figure(9):** Effect of  $D$  and  $\zeta$  on the temperature profile ( $n=0.5, I=1, R=V=0$ ).

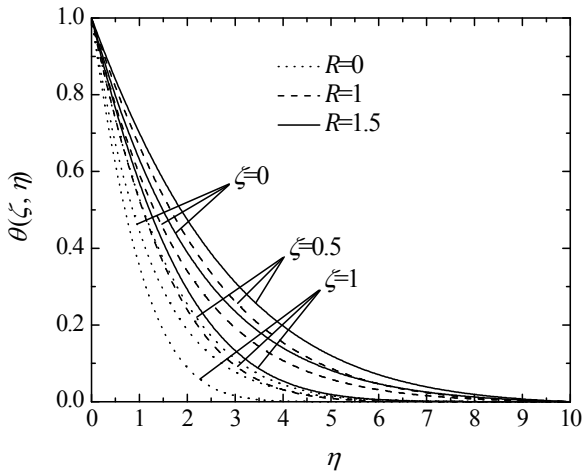
extracted from the plate. This require an increase in the local Nusselt number as shown in Figure (10).



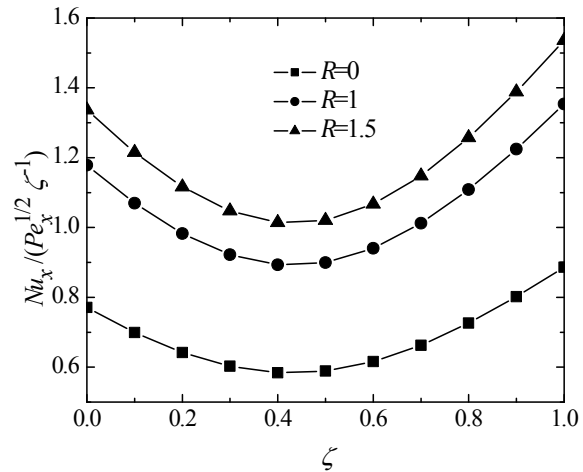
**Figure(10):** Effect of  $D$  and  $\zeta$  on the local Nusselt number ( $n=0.5, I=1, R=V=0$ ).



**Figure(11):** Effect of  $R$  and  $\zeta$  on the velocity profile ( $n=0.5, I=D=V=0$ ).



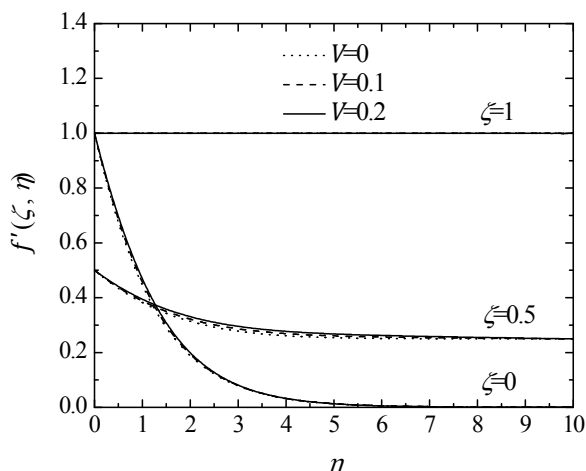
**Figure(12):** Effect of  $R$  and  $\zeta$  on the temperature profile ( $n=0.5, I=D=V=0$ ).



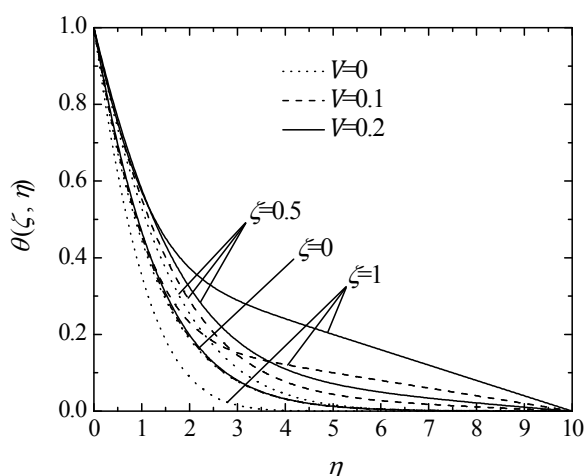
**Figure(13):** Effect of  $R$  and  $\zeta$  on the local Nusselt number ( $n=0.5, I=D=V=0$ ).

**Effect of  $R$ :** Non-dimensional velocity and temperature profiles inside the boundary layer are plotted in Figures (11) and (12) respectively. The velocity field is increased as the value of the radiation parameter is increased. This means that the effect of thermal radiation is to increase the convective moment in the boundary layer. It is observed that the thermal boundary-layer thickness increased with an increase in the value of the radiation parameter. This is because the temperature of the fluid in the medium increased due to the presence of thermal radiation. The variation of local Nusselt number with  $\zeta$  for different values of  $R$  is shown in Figure (13). The local Nusselt number increased with the increasing values of the radiation parameter. Also, the effect of radiation is to enhance the heat transfer coefficient in the medium.

**Effect of  $V$ :** The Non-dimensional velocity and temperature distribution across the boundary layer are plotted in Figures (14) and (15) respectively. From these figures it is evident that as the viscous dissipation increases the flow velocity and fluid temperature are increases. The increase in the temperature is due to internal heating associated with viscous dissipation. As stated previously the present study neglects the no-slip boundary conditions, due to which the local heat flux across the boundary layer is reduced. Figure (16) presented the behavior of the local Nusselt number with  $\zeta$  as  $V$  increases. It is clear that as  $V$  increases the local Nusselt number decreases. Due to the decrease in the temperature difference near the wall and in the porous medium, the viscous dissipation is decrease the local Nusselt number.

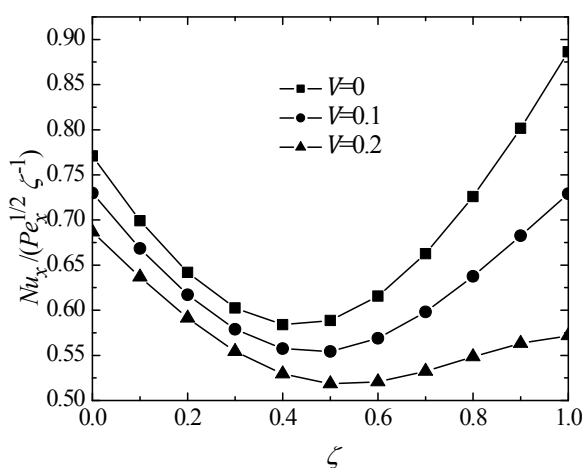


**Figure(14):** Effect of  $V$  and  $\zeta$  on the velocity profile ( $n=0.5, I=D=R=0$ ).

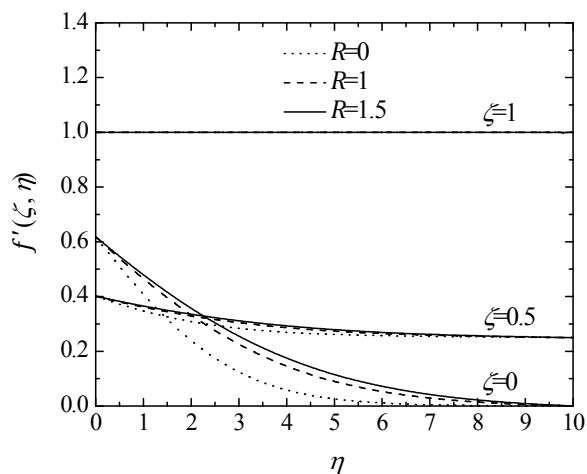


**Figure(15):** Effect of  $V$  and  $\zeta$  on the temperature profile ( $n=0.5, I=D=R=0$ ).

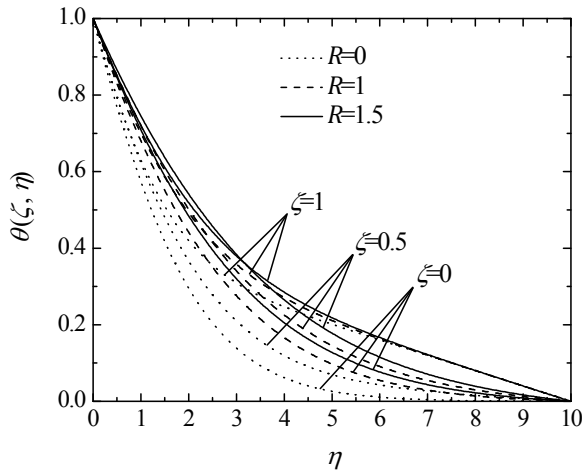
**Effect of  $R$  in the presence of  $IDV$  :** The effect of  $R$  and  $\zeta$  on the velocity and temperature profiles as well as the local Nusselt number are illustrated in Figures (17-19) respectively. From these figures it is evident that the behavior of the curves presents a similar trends to its counterpart in Figures (11-13) with the reduction in the velocity of fluid in Figure (17) as compared to Figure (11). The increase in the temperature of fluid in Figure (18) as compared to Figure (12). This leads to the reduction in the values of local Nusselt number in Figure (19) as compared to Figure (13).



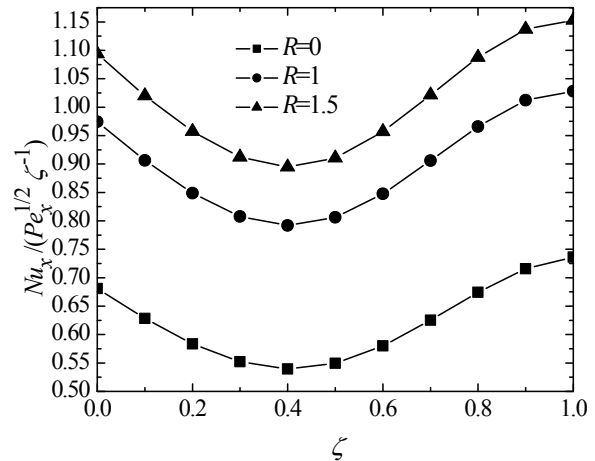
**Figure(16):** Effect of  $V$  and  $\zeta$  on the local Nusselt number ( $n=0.5, I=D=R=0$ ).



**Figure(17):** Effect of  $R$  and  $\zeta$  on the velocity profile ( $n=0.5, I=1, D=2, V=0.1$ ).



**Figure(18):** Effect of  $R$  and  $\zeta$  on the temperature profile ( $n=0.5, I=1, D=2, V=0.1$ ).



**Figure(19):** Effect of  $R$  and  $\zeta$  on the local Nusselt number ( $n=0.5, I=1, D=2, V=0.1$ ).

## Conclusions

From the present results it can be concluded that :

- 1- As  $n$  increases the local Nusselt number increases.
- 2- As  $I$  increases the local Nusselt number decreases.
- 3- As  $D$  increases the local Nusselt number increases.
- 4- The local Nusselt number increased with the increasing values of  $R$ .
- 5- The local Nusselt number decreases as  $V$  increases.
- 6- In the presence of  $nIDV$  as  $R$  increases the local Nusselt number increases.

## References

1. Yih, K. A., " Coupled Heat and Mass Transfer in Mixed Convection over a Vertical Flat Plate Embedded in Saturated Porous Media : PST/PSC or PHF/PMF, " Heat and Mass Transfer, Vol. 34, PP. 55-61, 1998.
2. Chamkha, A. J. and Khaled, A. –R. A., " Hydromagnetic Simultaneous Heat and Mass Transfer by Mixed Convection from a Vertical Plate Embedded in a Stratified Porous Medium with Thermal Dispersion Effects, " Heat and Mass Transfer, Vol. 36, PP. 63-70, 2000.
3. Aydin, O. and Kaya, A., " Non-Darcian Forced Convection Flow of Viscous Dissipating Fluid over a Flat Plate Embedded in a Porous Medium, " Transp Porous Med, Vol. 73, PP. 173-186, 2008.
4. Hung, Y. –M. and Tso, C. P., " Effects of Viscous Dissipation on Fully Developed Forced Convection in Porous Media, " International Communications in Heat and Mass Transfer, Vol. 36, PP. 597-603, 2009.
5. Chamkha, A. J., " Mixed Convection Flow Along a Vertical Permeable Plate Embedded in a Porous Medium in the Presence of a Transverse Magnetic Field, " Numerical Heat Transfer, Part A, Vol. 34, PP. 93-103, 1998.
6. Tashtoush, B. and Kodah, Z., " No Slip Boundary Effects in Non-Darcian Mixed Convection from a Vertical Wall in Saturated Porous Media. Analytical Solution, " Heat and Mass Transfer, Vol. 34, PP. 35-39, 1998.

7. Kodah, Z. H. and Al-Gasem, A. M., " Non-Darcy Mixed Convection from a Vertical Plate in Saturated Porous Media-Variable Surface Heat Flux, " *Heat and Mass Transfer*, Vol. 33, PP. 377-382, 1998.
8. Gorla, R. S. R. and Kumari, M., " Nonsimilar Solutions for Mixed Convection in Non-Newtonian Fluids Along a Vertical Plate in a Porous Medium, " *Transport in Porous Media*, Vol. 33, PP. 295-307, 1998.
9. Hassanien, I. A., Bakier, A. Y., and Gorla, R. S. R., " Effects of Thermal Dispersion and Stratification on Non-Darcy Mixed Convection from a Vertical Plate in a Porous Medium, " *Heat and Mass Transfer*, Vol. 34, PP. 209-212, 1998.
10. Murthy, P. V. S. N., " Thermal Dispersion and Viscous Dissipation Effects on Non-Darcy Mixed Convection in a Fluid Saturated Porous Medium, " *Heat and Mass Transfer*, Vol. 33, PP. 295-300, 1998.
11. Chamkha, A. J. and Khaled, A. -R. A., " Nonsimilar Hydromagnetic Simultaneous Heat and Mass Transfer by Mixed Convection from a Vertical Plate Embedded in a Uniform Porous Medium, " *Numerical Heat Transfer, Part A*, Vol. 36, PP. 327-344, 1999.
12. Tashtoush, B., " Analytical Solution for the Effect of Viscous Dissipation on Mixed Convection in Saturated Porous Media, " *Transport in Porous Media*, Vol. 41, PP. 197-209, 2000.
13. Hassanien, I. A. and Omer, Gh. M., " Nonsimilarity Solutions For Mixed Convection Flow Along Non-isothermal Vertical Plate Embedded in Porous Media with Variable Permeability, " *Journal of Porous Media*, Vol. 5, No. 2, PP. 159-167, 2002.
14. Chamkha, A. J., Takhar, H. S., and Beg, O. A., " Numerical Modelling of Darcy-Brinkman-Forchheimer Magnetohydrodynamic Mixed Convection Flow in a Porous Medium with Transpiration and Viscous Heating, " *International Journal of Fluid Mechanics Research*, Vol. 29, No. 1, PP. 1-26, 2002.
15. Murthy, P. V. S. N., Mukherjee, S., Srinivasacharya, D., and Krishna, P. V. S. S. R., " Combined Radiation and Mixed Convection from a Vertical Wall with Suction/Injection in a Non-Darcy Porous Medium, " *Acta Mechanica*, Vol. 168, PP. 145-156, 2004.
16. Mohammadein, A. A. and El-Shaer, N. A., " Influence of Variable Permeability on Combined Free and Forced Convection Flow Past a Semi-Infinite Vertical Plate in a Saturated Porous Medium, " *Heat and Mass Transfer*, Vol. 40, PP. 341-346, 2004.
17. Reddy, P. B. A. and Reddy, N. B., " Radiation Effects on MHD Combined Convection and Mass Transfer Flow Past a Vertical Porous Plate Embedded in a Porous Medium with Heat Generation, " *Int. J. of Appl. Math and Mech*, Vol. 6, No. 18, PP. 33-49, 2010.
18. Bejan, A., " *Convection Heat Transfer*, " Second Edition, John Wiley & Sons, Inc., 1995.
19. Mansour, M. A. and Gorla, R. S. R., " Mixed Convection-Radiation Interaction in Power-Law Fluids Along a Non-isothermal Wedge Embedded in a Porous Medium, " *Transport in Porous Media*, Vol. 30, PP. 113-124, 1998.
20. Ingham, D. B. and Pop, I., " *Transport Phenomena In Porous Media II*," Pergamon, 2002.
21. Hsieh, J. C., Chen, T. S., and Armaly, B. F., " Mixed Convection Along a Non-Isothermal Vertical Flat Plate Embedded in a Porous Medium : The Entire Regime, " *Int. J. of Heat and Mass Transfer*, Vol. 36, Issue 7, PP. 1819-1825, May 1993.
22. Narayana, M., Khidir, A. A., Sibanda, P., and Murthy, P. V. S. N., " Viscous Dissipation and Thermal Radiation Effects on Mixed Convection from a Vertical Plate in a Non-Darcy Porous Medium, " Vol. 96, PP. 419-428, 2013.

**The work was carried out at the college of Engineering. University of Mosul**